A New Cooperative Control Solution of Subway BAS: An Improved Fuzzy PID Control Algorithm

Hui Fang [Corresp., 1, 2] , **Shusong Yang** [1] , **Ying Shi** [3] , **Yang Wang** [1] , **Yue Jiang** [1] , **Chaochao Song** [3] , **Wei Zhang** [Corresp. 2]

[1] Ningbo Rail Transit Group Co., Ltd., Ningbo, Zhejiang, China

[2] Zhejiang University, Hangzhou, Zhejiang, China

[3] New Business Incubation Department, ZheJiang SUPCON Technology Co., Ltd, Hangzhou, Zhejiang, China

Corresponding Authors: Hui Fang, Wei Zhang
Email address: stheseus@126.com, zwei9876@163.com

The building automation system (BAS) of a subway is the core component of monitoring and managing urban rail transit systems. For the current problems such as low control efficiency, insufficient accuracy, and poor stability of metro BAS, this paper proposes a cooperative control framework based on an improved fuzzy PID algorithm. Firstly, the concept of an integrated supervisory control system (ISCS) for subways is introduced by summarizing the previously implemented engineering construction and combining it with advanced automation technology. The system's overall design under the ISCS framework is also improved by integrating it with the fire alarm system (FAS) with the BAS as the core unit of the reliance. Then, an improved seeker optimization algorithm (ISOA) is employed to optimize the parameters of the fuzzy PID control algorithm to achieve a coordinated control of the system based on considering the time lag problem. Finally, the accuracy, efficiency, and stability of the coordinated control response of the BAS under the ISCS framework are tested experimentally. The results suggest that the proposed cooperative control solution of BAS employing the improved fuzzy PID algorithm has good control accuracy and response efficiency and can also ensure the BAS's higher stability in the coordinated control process, which thus greatly improves the automation level of the subway and provides a safer and more reliable high-performance for the ISCS of the subway in the urban rail transportation industry.

1   # A New Cooperative Control Solution of Subway BAS: An Improved

2   # Fuzzy PID Control Algorithm

4   Hui Fang[1*,2], Shusong Yang[2], Ying Shi[3], Yang Wang[2], Yue Jiang[2], Chaochao Song[3], Wei

5   Zhang[1*]

7   [1]Zhejiang University, Hangzhou, Zhejiang, China

8   [2]Ningbo Rail Transit Group Co., Ltd., Ningbo, Zhejiang, China

9   [3]New Business Incubation Department, Zhejiang SUPCON Technology Co., Ltd, Hangzhou,

10   Zhejiang, China

11   * Corresponding author: Hui Fang, Email: stheseus@126.com; Wei Zhang, Email:

12   zwei9876@163.com

13   Note * denotes the authors are co-corresponding authors of the article.

15   **Abstract:** The building automation system (BAS) of a subway is the core component of monitoring and managing

16   urban rail transit systems. For the current problems such as low control efficiency, insufficient accuracy, and poor

17   stability of metro BAS, this paper proposes a cooperative control framework based on an improved fuzzy PID

18   algorithm. Firstly, the concept of an integrated supervisory control system (ISCS) for subways is introduced by

19   summarizing the previously implemented engineering construction and combining it with advanced automation

20   technology. The system's overall design under the ISCS framework is also improved by integrating it with the fire

21   alarm system (FAS) with the BAS as the core unit of the reliance. Then, an improved seeker optimization algorithm

22   (ISOA) is employed to optimize the parameters of the fuzzy PID control algorithm to achieve a coordinated control

23   of the system based on considering the time lag problem. Finally, the accuracy, efficiency, and stability of the

24   coordinated control response of the BAS under the ISCS framework are tested experimentally. The results suggest

25   that the proposed cooperative control solution of BAS employing the improved fuzzy PID algorithm has good control

26   accuracy and response efficiency and can also ensure the BAS's higher stability in the coordinated control process,

27   which thus greatly improves the automation level of the subway and provides a safer and more reliable high-

28   performance for the ISCS of the subway in the urban rail transportation industry.

29   **Keywords:** BAS; Dynamic optimization algorithm; fuzzy PID control algorithm; cooperative control solution

30   # 1 Introduction

31   The construction of subways has stepped into a rapid development phase since its fast and efficient urban public

32   transportation saves time and money for millions. As an important means for each city to resolve the traffic congestion

33   problem led by rapidly expanded urban areas and to boost domestic demand to accelerate economic growth are some

34   leading advantages. The internal system of the subway has also received growing attention [1-2]. The subway is

35   generally built below the ground. Commuters gather in public spaces whose carrying capacities are relatively limited.

36   Several electromechanical equipment are located in the stations and subway zones. Those facilities help commuters

37   travel safely and comfortably, and traffic flowing in stations continues smoothly due to their operational capability.

38   Many types and numbers of electromechanical equipment with complicated control processes are distributed along

39   the line. The BAS is an automatic control system based on the theory of ventilation, air conditioning, and disaster

40   prevention in the subway system that combines computer and network technology with the principle of automatic

41   control of electromechanical equipment and uses a distributed microcomputer monitoring system. The main

42   functionalities are air conditioning and ventilation, lighting, water supply and drainage, escalators, elevators, and

43   guidance signs in subway stations and tunnels [3]. Thus, passengers travel safely and comfortably while ensuring the

44   safety and security of the stations. However, various scattered devices in the current subway system and the existing

45   BAS often have difficulty responding quickly to the actual changes in the subway stations since low control accuracy

46   and poor stability mainly appear as the main issues. With the increasing demand for metro automation control, the

47   realization of intelligent coordinated control of metro BAS has become a key research direction for both academia

48   and industry [4].

49   In recent years, as computerized systems have advanced, control and network communication technologies have been

50   employed by domestic and foreign metro companies that used hot standby redundant PLC to build BAS by utilizing

51   metro design specifications [5-7]. The scientific and reasonable integration and interconnection of relevant subsystems

52   in ISCS is essential for the system hardware, software platforms, and network construction [8-10]. From the current

53   status of a subway BAS implementation, the structure of a subway ISCS depends on its data service mode since both

54   comparison and analysis of the subway lines in different periods are required. In the past, the centralized ISCS mainly

55   relied on the performance of the central-level server. Then, the central server and the network carried a large burden,

56   which could easily cause the paralysis of the whole line in case major accidents or occurrences happened [11-13].

57   With the rapid development of network technology, a distributed ISCS has been used in large numbers in the current

58   metro industry and has become the current development direction of the urban rail transit industry.

59   Further study reveals that BAS and FAS are set up independently in a conventional scheme, i.e., the two systems are

60   configured with various devices at the central control level and station level and use independent transmission channels

61   for information sharing. Each system performs its monitoring separately. Hence, an integrated BAS and FAS, which

62   cooperate and coordinate with each other in practice, are characterized as complementary and dependent whereas a

63   single system cannot control the whole process. The ISCS has access to the professional data of the subsystem of the

64   subway station, which can fully combine the information of trains entering and leaving stations and the pedestrian

65   flow, as well as the information of the subway obtained by BAS sensors, to perform periodic controls of the automatic

66   adjustment and the electromechanical equipment. Thus, the purpose of reducing energy consumption and providing

67   passengers with a high-quality riding environment could be achieved. Therefore, it is of great significance for

68   engineering practices and economic value to study the coordinated control framework of metro BAS when the ISCS

69   is under consideration.

70   The paper is divided into five main parts: the first part is the introduction, the second part is the design of a BAS

71   coordination control framework when the ISCS framework is considered, the third section is the application of the

72   fuzzy PID control algorithm and its optimization in a BAS coordination control framework, the fourth section is the

73   experimental validation, and the fifth part is the conclusion and future work.

2 The design of a BAS coordination control framework under the ISCS framework

2.1 The general structure of the ISCS

As a comprehensive information platform, ISCS integrates the central-level functions of several subsystems such as signaling and automatic ticketing to master the operation of the whole line equipment and is also responsible for monitoring and dispatching the equipment within its assessment and maintenance personnel. The ISCS can monitor the operation status and fault situations of the equipment under the assessment of each station system of the whole line. Issues are instructed to each station to unify the command and coordinate the operation of each station.

The overall structure of the ISCS is designed based on the principles of two levels of management (central, station) and three levels of control (central, station, site), as shown in Figure 1.

Figure 1: The general structure of the ISCS.

The ISCS is divided into three layers from the configuration of hardware equipment.

    1) Central-level Integrated Supervisory Control System (CISCS).

    2) Station-level Integrated Supervisory Control System (SISCS).

    3) Site-level control equipment (integrated subsystem part).

2.2 The overview of the coordination control framework

BAS generally consists of the BAS equipment installed in the station's electric control rooms and other related components such as vehicle sections and on-site BAS equipment. BAS equipment is composed of a redundant station controller (PLC controller), BAS bus network, remote IO, and IBP disk PLC.

The PLC near the station control room (end A) is the master controller and the PLC at the other end (end B) is the slave controller. The PLCs at the two ends are connected by redundant buses, and various types of RI/O, site devices with intelligent communication ports, and local site mini-controllers are connected to monitor and manage the electromechanical equipment (HVAC, escalators, low-voltage lighting, water supply, and drainage) at the two ends of the station, respectively.

In the fire mode, the FAS sends a command to the BAS, and the BAS controller will start the relevant equipment in a disaster mode according to the predefined working conditions. Then, the station control room has an integrated backup panel (IBP) set up by the integrated monitoring system as an emergency backup control in a disaster mode. The BAS has a single PLC in the IBP panel, which requires high reliability and real-time operation of the BAS and requires the system response faster and more accurate as shown in Figure 2.

Figure 2: The actual control structure of the ISCS.

2.3 The architecture of the framework of the coordination control

The BAS adopts a two-level management and three-level control architecture, i.e. two-level management at the control center and station (vehicle section and parking lot), and three-level control at the control center (vehicle section, station, and parking lot). The BAS is integrated into the comprehensive monitoring system at the station level, which realizes its functions at the central and station levels, respectively. The BAS comprises rooms such as control,

112 monitoring equipment, station control, vehicle section, parking lot, and other on-site BAS equipment. The control
113 structure of a BAS is shown in Figure 3.

114

115   **Figure 3: The control structure of the BAS.**

116

117 Two sets of redundant G5pro PLCs are installed in the loop control rooms at each end of the station, with the PLC
118 near the station control room (end A) as the master controller and the PLC at the other end (B end) as the slave
119 controller. The PLCs at both ends of the station are connected to the Ethernet ring network. All kinds of RI/O and
120 field devices with intelligent communication ports are connected to monitor and manage the electromechanical
121 equipment (ventilation and air conditioning, lighting, directional signs, escalators, elevators, human-proof doors
122 (flood-proof doors) and water supply and drainage systems at both ends of the station. The architecture of the
123 coordinated control framework of a BAS is shown in Figure 4.

124

125   **Figure 4: The architecture of the framework of the coordinated control for the BAS.**

126

127 The BAS station is equipped with a special COM5004RTU communication module connected to the FAS station for
128 communication. In the fire mode, the FAS sends a command to the BAS, and the BAS controller will switch to the
129 disaster mode and activate the relevant equipment according to the predetermined working conditions. The station
130 control room has an IBP set up by the integrated monitoring system as an emergency backup control in disaster mode.
131 The BAS site-level monitoring system mainly includes a redundant GCU5001-S controller as the BAS redundant
132 controller, and the site-level monitoring equipment is configured according to the installation of mechanical and
133 electrical equipment. The G5pro series remote intelligent RI/O is equipped to communicate with the redundant
134 GCU5001-S controller through the network.
135 The main PLC controller of the underground station is equipped with two redundant EtherNet/IP Ethernet
136 communication interfaces (redundant COM5002TCP modules) to communicate with the redundant switches of the
137 integrated monitoring system. The GCU5001-S PLC controllers at both ends of the station communicate with the
138 Ethernet ring network by using fiber optic media. The GCU5001-S PLC controllers communicate with the G5pro
139 series remote I/O modules. GCU5001-S PLC controller and G5pro series remote I/O, frequency converter, intelligent
140 low-voltage, etc., are connected by a ring network. The BAS redundant GCU5001-S PLC controller is connected to
141 the FAS via the RS485 bus. The IBP disk GCU5001-S PLC is connected to the master and slave GCU5001-S PLC
142 controllers via the Ethernet ring network.

143 3 The improved fuzzy PID control algorithm

144 3.1 Fuzzy PID control algorithm

145 Fuzzy control is a nonlinear control method, which has the advantages of not requiring an exact mathematical
146 functional model, high stability, strong robustness, and better control systems containing PLCs. Therefore, to achieve
147 the coordinated control of a BAS, this paper adopts the fuzzy PID control algorithm as the basic control algorithm of
148 a BAS.
149 The system structure of the fuzzy PID controller is shown in Figure 5. The system mainly consists of two parts: PID
150 control and fuzzy control. R_p denotes the preset coordinated control response effect, and R_a represents the coordinated

151 control response effect in actual action, and the error ε and the change error rate ε_c are used as the input signals of the

152 fuzzy controller [14-15].

153

154 **Figure 5: The system structure of the fuzzy PID controller.**

155

156 The PID controller output value is calculated by using Eq. (1) [16].

157
$$u(t) = k_p \left[e(t) + k_i \int_0^t e(t)dt + k_d \frac{d\varepsilon(t)}{dt} \right] \tag{1}$$

158 where $u(t)$, k_p, k_i, and k_d denote controller output value, proportionality, integration, and differentiation coefficients,

159 respectively in Eq. (1).

160 When the BAS responds to the coordinated control command, it detects the response error ε and the change error rate

161 ε_c in real-time and then finds the optimal solution for adjusting the PID control parameters of Vk_p, Vk_i, and Vk_d

162 according to the fuzzy rules in real-time. The system response is fast and smooth. The adjustment is shown in Eq. (2)

163 [17].

164
$$\begin{cases} k_p = k_{p1} + Vk_p \\ k_i = k_{i1} + Vk_i \\ k_d = k_{d1} + Vk_d \end{cases} \tag{2}$$

165 In Eq. (2), k_{p1}, k_{i1} and k_{d1} are the initial values of the PID control parameters of k_p, k_i, and k_d, respectively. The

166 theoretical domain of the input variables' errors ε and change error rate ε_c is contained in [-6, 6], and the theoretical

167 domain of the output variables adjusted by the PID control parameters of Vk_p Vk_d is contained in [-1, 1]. The fuzzy

168 subsets are described in fuzzy language as positive big (PB), positive medium (PM), positive small (PS), zero (ZO),

169 negative small (NS), negative medium (NM), and negative big (NB) to facilitate data processing. Each fuzzy subset

170 uses the triangular affiliation function corresponding to each fuzzy subset.

171 To ensure the reliability and stability of the whole system, reasonable fuzzy rules are proposed as follows:

172 (1) When ε and ε_c are small or equal to 0, k_p takes a large value, k_i takes a large value, and k_d takes a medium

173 value.

174 (2) When ε and ε_c are large, k_p takes a large value, k_i takes a zero value, and k_d takes a small value.

175 (3) When ε and ε_c are equal in size, k_p takes a small value, k_i takes a moderate value, and k_d takes a moderate

176 value.

177 According to the above fuzzy rules, the fuzzy control rules are established as shown in Table 1.

178 **Table 1: The control table of fuzzy rules.**

179 ## 3.2 The ISOA-optimized fuzzy PID controller.

180 SOA is a new swarm intelligent evolutionary algorithm that can find the optimal solution to a target by simulating the

181 human search behavior for both the position and direction in space [18]. In the conventional fuzzy PID control, the

182 quantization and scaling factors must be set according to the expert's experience and cannot be adjusted adaptively

183 when they are set. Thus, poor settings of these parameters could lead to oscillation and overshoot of the system, which

184 cannot adapt to the random errors and disturbances existing in the actual regulation and control, and the steady-state

185 performance becomes poorer. To improve the performance of the fuzzy PID controller, the SOA is employed for both

186 the input and output processes of the fuzzy controller.

187 The SOA provides a basic principle. Suppose that a population has S search individuals distributed in a D-dimensional

188 space. Everyone is equipped with both position and direction information. Through multiple search updates, the

189 individual obtains both the optimal position and direction in the space to attain the objective function's optimal

190 solution. The position of individual X_i is shown in Eq. (3) [19].

191
$$X_i = \left[x_i, x_{i2}, \mathsf{L}, x_{in} \right]^p \tag{3}$$

192 Each individual in the group possesses three search behaviors, which are co-altruistic behavior $\vec{d}_{i,\text{coa}}$, altruistic

193 behavior $\vec{d}_{i,\text{alt}}$, and proactive behavior $\vec{d}_{i,\text{pro}}$.

194
$$\begin{cases} \vec{d}_{i,\text{coa}}(t) = \vec{P}_{i,\text{best}} - \vec{x}_i(t) \\ \vec{d}_{i,\text{alt}}(t) = \vec{g}_{i,\text{best}} - \vec{x}_i(t) \\ \vec{d}_{i,\text{pro}}(t) = \vec{x}_i(t_1) - \vec{x}_i(t_2) \end{cases} \tag{4}$$

195 where $\vec{x}_i(t), \vec{P}_{i,\text{best}}$, and $\vec{g}_{i,\text{best}}$ represents individual current best position, individual historical best position, and

196 group best position in the neighborhood, respectively, and $\vec{x}_i(t_1), \vec{x}_i(t_2)$ are delineated as the current moment as the

197 previous reference moment and best position of the two moments before the current moment are defined.

198 Once the three search behaviors of an individual are calculated, the position can be updated iteratively according to the individual's

199 final search direction. The iterative update of the position according to the final search direction of the individual is presented in

200 Eq. (5) [20].

201
$$\begin{cases} \vec{d}_{id}(t) = sign\left[\omega \vec{d}_{id,\text{pro}} + 0.5 \vec{d}_{id,\text{ego}} + 0.5 \vec{d}_{id,\text{alt}}(t) \right] \\ \Delta x_{id}(t+1) = a_{id} d_{id}(t) \\ x_{id}(t+1) = x_{id}(t) + \Delta x_{id}(t+1) \end{cases} \tag{5}$$

202 where ω representing inertia weight determines the direction of the individual's self-interested movement at the next moment,

203 $\vec{d}_{id}(t)$ shows the direction of the individual's search at the next moment, a_{id} represents the search step determined by the Gaussian

204 affiliation function, and $x_{id}(t+1)$ denotes the location of the individual at the next moment.

205 To evaluate the merit of the solution in the search evolution process, the ITAE performance index is chosen as the minimum

206 objective function, where the squared input term $u^2(t)$ is added to reduce the overshoot and oscillation of the system, and the specific

207 fitness function is presented in Eq. (6).

208
$$F = \int_0^\infty \left(\omega_1 | e(t) | \right) + \omega_2 u^2(t) \mathrm{d}t \tag{6}$$

209 where ω_1 and ω_2 take 0.9 and 0.1, respectively.

210 In the SOA, inertia weights play an important role in the search direction of individuals. When the individual target values are not

211 attained, the individual search ability becomes poor, and the inertia weight should be increased to improve the global search ability.

212 When the individual search values are scattered, the weight should be reduced to speed up the convergence. However, the inertia

213 weight ω is generally fixed in the standard SOA, and this strategy will not be able to cope with the random disturbance factors of

214 the fuzzy control process. Therefore, this paper improves the SOA by utilizing a weight factor with adaptive characteristics to

215 search for the best. Eq. (7) presents it.

216
$$\omega = \begin{cases} \omega_{\min} + \dfrac{\left(\omega_{\max} - \omega_{\min} \right) \cdot \left(f - f_{\min} \right)}{f_{\text{avg}} - f_{\min}}, f, f_{\text{avg}} \\ \\ \omega_{\max} \end{cases} \tag{7}$$

217 where $\omega_{\max}$ and $\omega_{\min}$ show the maximum and minimum values of the inertia weights, respectively, f, $f_{\min}$, and f_{avg} designates

218 the current target fitness value, the minimum value of fitness in the current group of individuals, and the mean value of fitness in

219   the current group of individuals, respectively.

220   When the calculated fitness score is lower than the population mean, the adaptive weight ω is employed for iteration; otherwise

221   ω_{max} is chosen as the individual iteration weights that can be adaptively adjusted according to the changes in the population fitness

222   values. More up-to-date research can be found [21-23]

3.3 Design of the ISOA-Fuzzy PID Controller

224   The structure of the ISOA-fuzzy PID control can be obtained from Subsection 3.2, as shown in Figure 6.

226   **Figure 6: The structure of the ISOA-fuzzy PID control-based.**

228   Based on the above study, a BAS controller with the SOA-optimized fuzzy PID is designed, and the specific steps are presented as

229   follows:

230   Step 1: Initialize the search population, set the SOA individual size N as 50, set the individual search space dimension D as 5,

231   represent the quantization factor and scale factor of fuzzy control, set the individual search range as [0,5], set the maximum number

232   of iterations M as 50, set the minimum fitness value f as 0.1, and set the inertia weights ω_{max} and ω_{min} as 0.9 and 0.1, respectively.

233   Step 2: Call the BAS fuzzy PID module to obtain the fitness value of each individual in the current iteration and determine whether

234   the abort condition (the maximum number of iterations or the minimum fitness value) is satisfied.

235   Step 3: Calculate the maximum and mean values of the population fitness in the current iteration and assign adaptive inertia weights

236   ω to each of the N individuals according to Eq. (4).

237   Step 4: Update both the orientation and position of individuals according to Eq. (5) and go back to Step 2.

238   The coordinated control flow of the BAS with the SOA-optimized fuzzy PID is shown in Figure 7.

240   **Figure 7: The coordinated control flow of the BAS with the ISOA-optimized fuzzy PID.**

4 Solution Testing

242   To analyze the performance of the ISOA-optimized fuzzy PID control model in the BAS coordinated control framework, the

243   Simulink module in MATLAB 2017 is conducted to run simulation and comparison experiments, which is shown in Figure 8.

245   **Figure 8: The BAS coordinated control module.**

247   This model sets the system input to a first-order step response. Running simulations lead the ISCS to send the command to the

248   preset -value. The system response curves for the Fuzzy-PID, SOA-Fuzzy-PID, and ISOA-Fuzzy-PID control methods are shown

249   in Figure 9.

250   According to the response curve in Figure 10, the Fuzzy-PID control is applied to BAS. When the coordinated control is applied

251   to BAS, a faster rise process is observed, and the preset value is reached first. However, due to the nonlinearity of the controlled

252   object, the Fuzzy-PID control is prone to overshoot, and the final overshoot is 14.6%, the regulation time is 47.1 seconds, and the

253   steady-state error is 0.8%, so the system performance and the steady-state performance are poor. The overshoot of the SOA-Fuzzy-

254   PID model is 4.1% and the adjustment time is 26.4 seconds. Although this model can effectively suppress the overshoot, a slow

255   rise process appears and the parameters in the controller still need to be adjusted empirically, so the adaptive capability is not good.

256   The ISOA-Fuzzy-PID model has no overshoot in the control process, and when compared with the SOA-Fuzzy-PID, the overshoot

257   is reduced by 4.1% and the regulation time is shortened by 27.8%, so its control performance is the best. The specific performance

258   indexes of the three control methods are shown in Table 2.

259

260   **Figure 9: The system response curves for the fuzzy PID, SOA-PID, and ISOA-PID control methods.**

261   **Table 2: The contrasts of various performance indicators of the control system.**

262

263   **Figure 10: The step response curve of the proposed system with interference.**

264

265   To verify the stability and adaptive capability of the ISOA-Fuzzy-PID model when applied to the BAS coordinated control,

266   disturbance signals, and Gaussian random signals are introduced to simulate the response after the change of real environment

267   parameters. Figure 11 shows the step response curves of the three control systems with the introduction of disturbances at 80

268   seconds after the output stabilization. Figure 9 depicts that after introducing an 8% disturbance of the preset value, the ISOA-

269   Fuzzy-PID controller returns to the steady state after 10 seconds, while the SOA-Fuzzy-PID and the Fuzzy-PID return to the

270   constant state after 21 and 26 seconds, respectively.

271

272   **Figure 11: The step response curve of the system with a high-frequency signal.**

273   Figure 11 shows the output curves of the three control methods after introducing the Gaussian random signal, where the mean and

274   the variance of the signal are set to 1 and 0.1, and the sampling time is 25 seconds, respectively. Figure 11 shows that the ISOA-

275   fuzzy PID controller has better regulation ability, curve tracking, and steady-state performance than the fuzzy PID and the SOA-

276   PID after introducing a Gaussian random signal.

277   In summary, the ISOA-PID control model adopted in this paper can effectively realize accurate and fast responses employing the

278   BAS coordinated control, contributing to the safe and stable operation under the ISCS framework.

279   5 Conclusion

280   In this paper, the metro BAS control method employing the ISOA-optimized fuzzy PID is adopted based on the excellent merit-

281   seeking capability of the SOA algorithm after the SOA is improved. The experiments show that the optimization of the quantization

282   and scaling factors of the fuzzy controller by utilizing the intelligent optimization method can improve the performance of the

283   system control while avoiding over-reliance on the expert experience. According to the performance indexes of the simulation

284   results, the ISOA-Fuzzy-PID control reduces the regulation time and overshoot when compared with Fuzzy-PID and Fuzzy-PID in

285   the BAS coordinated control processes. The system can be adjusted to the steady state first after introducing disturbances and high-

286   frequency signals, suggesting that the model has high control accuracy and steady-state performance and provides a reference value

287   for the current metro BAS design.

288   The model is proven to have increased control accuracy and steady-state performance, which provides some reference value for

289   the current subway BAS design. Besides, it is worth noting that the actual ISCS modeling of the metro needs to consider multiple

290   environmental factors, and disaster data still needs to be further collected. However, the experimental tests are not conducted in

291   this paper due to not collecting enough data for the research. In the next phase of the research, we plan to practically test the

292   performance of the proposed method for the application of coordinated control of the BAS in the ISCS in the subway.

293   References

294   [1]   J. Yu, P. Tian, H. Feng, and Y. Xiao, "Research and Design of Subway BAS Intrusion Detection Expert System," 2018 IEEE

295   3rd Advanced Information Technology, Electronic and Automation Control Conference (IAEAC), Chongqing, China, 2018,

296   pp. 152-156.

297   [2]   C. Zhixin, Z. Changgen, W. Jia and W. Xiaohui, "Communication in BAS Network System in Subway Station," 2010
298   International Conference on Computational Aspects of Social Networks, Taiyuan, China, 2010, pp. 679-682.

299   [3]   W. Jia, L. Shufeng, C. Zhixin and W. Xiaohui, "Network Analysis of Underground Transportation Hub Safety Monitoring
300   System," 2010 International Conference on Computational Aspects of Social Networks, Taiyuan, China, 2010, pp. 629-632.

301   [4]   T. Guo, T. Han and J. Li, "Functional Design on the Building Automation System of Subways Based on CIMS," 2010 2nd
302   International Workshop on Intelligent Systems and Applications, Wuhan, China, 2010, pp. 1-4.

303   [5]   B. A. D. J. C. K. Basnayake, Y. W. R. Amarasinghe, R. A. Attalage, A. G. B. P. Jayasekara, and M. G. K. Devinda,
304   "Development of multi-sensory feedback system for building automation systems," *2017 IEEE SENSORS*, Glasgow, UK,
305   2017, pp. 1-3.

306   [6]   A. Vallati, S. Grignaffini, M. Romagna and L. Mauri, "Effects of different building automation systems on the energy
307   consumption for three thermal insulation values of the building envelope," *2016 IEEE 16th International Conference on*
308   *Environment and Electrical Engineering (EEEIC)*, Florence, Italy, 2016, pp. 1-5.

309   [7]   Ohlenbusch, M., Bartner, N. F., Vöge, S., Vox, J. P., Fleßner, J., Frenken, M., & Wallhoff, F. (2018, August). Installation
310   and Control of Building Automation Systems Using Human-Robot-Interaction. In 2018 23rd International Conference on
311   Methods & Models in Automation & Robotics (MMAR) (pp. 493-497). IEEE.

312   [8]   W. Rajeh, "An Integrated Authentication Scheme for Supervisory Control and Data Acquisition System Based on Quantum
313   Key Distribution," *2022 2nd International Conference on Computing and Information Technology (ICCIT)*, Tabuk, Saudi
314   Arabia, 2022, pp. 374-378.

315   [9]   G. Ahmadi-Assalemi, H. Al-Khateeb, G. Epiphaniou and A. Aggoun, "Super Learner Ensemble for Anomaly Detection and
316   Cyber-risk Quantification in Industrial Control Systems," in *IEEE Internet of Things Journal*.

317   [10] M. Hussain, C. Fidge, E. Foo and Z. Jadidi, "Discovering Data-Aware Mode-Switching Constraints to Monitor Mode-
318   Switching Decisions in Supervisory Control," in *IEEE Transactions on Industrial Informatics*, vol. 18, no. 6, pp. 3734-3743,
319   June 2022.

320   [11] J. -J. Yan, G. -H. Yang and X. -X. Liu, "A Multi-Gain Switching Mechanism-Based Secure Estimation Scheme Against DoS
321   Attacks for Nonlinear Industrial Cyber-Physical Systems," in *IEEE Transactions on Industrial Electronics*, 2022.

322   [12] J. G. Chand, K. Susmitha, A. Gowthami, K. M. Chowdary and S. K. Ahmed, "IOT-Enabled Vertical Farming Monitoring
323   System Using Big Data Analytics," *2022 Second International Conference on Advances in Electrical, Computing,*
324   *Communication and Sustainable Technologies (ICAECT)*, Bhilai, India, 2022, pp. 1-6.

325   [13] R. Parveen and T. Nandan, "Developing a Testing Framework for Cyber-Physical Systems using Gazebo," *2022 IEEE*
326   *Workshop on Design Automation for CPS and IoT (DESTION)*, Milano, Italy, 2022, pp. 50-56.

327   [14] A. Laib, B. Talbi, A. Krama and M. Gharib, "Hybrid Interval Type-2 Fuzzy PID+I Controller for a Multi-DOF Oilwell Drill-
328   String System," in *IEEE Access*, vol. 10, pp. 67262-67275, 2022.

329   [15] M. Ahmadi Kamarposhti, H. Shokouhandeh, M. Alipur, I. Colak, H. Zare and K. Eguchi, "Optimal Designing of Fuzzy-PID
330   Controller in the Load-Frequency Control Loop of Hydro-Thermal Power System Connected to Wind Farm by HVDC Lines,"
331   in *IEEE Access*, vol. 10, pp. 63812-63822, 2022.

332   [16] B. Puviyarasi, C. Murukesh and K. Srividya, "Design and Implementation of PID Controller and Fuzzy Logic Controller for
333   Liquid Level System," *2022 8th International Conference on Advanced Computing and Communication Systems (ICACCS)*,
334   Coimbatore, India, 2022, pp. 1463-1466.

335   [17] J. Wang, Z. Lu, and G. Wang, "Design and Application of Temperature Control System Based on Fuzzy PID
336   Algorithm," *2022 7th International Conference on Intelligent Computing and Signal Processing (ICSP)*, Xi'an, China, 2022,
337   pp. 156-161.

338   [18]   X. Xiangrui, G. Jia, L. Zhuguan, L. Qianlin, and D. Hongwei, "DDPG-Based Improved Seeker Optimization Algorithm for
339   Robot Path Planning," *2022 2nd International Conference on Computer, Control, and Robotics (ICCCR)*, Shanghai, China,
340   2022, pp. 27-31.

341   [19]   S. Duan, H. Luo, and H. Liu, "A Multi-Strategy Seeker Optimization Algorithm for Optimization Constrained Engineering
342   Problems," in *IEEE Access*, vol. 10, pp. 7165-7195, 2022.

343   [20]   P. Ning, X. Pan, X. Xia, Q. Zhang, and L. Shen, "Application of SOA Optimization Back-stepping Control in Single Stage
344   Photovoltaic Inverter Control," *2021 4th International Conference on Energy, Electrical and Power Engineering (CEEPE)*,
345   Chongqing, China, 2021, pp. 576-580.

346   [21]   Z. Liu, Z. Liu, J. Liu, N. Wang, "Thermal management with fast temperature convergence based on optimized fuzzy PID
347   algorithm for the electric vehicle battery", Applied Energy, Volume 352, 2023, 121936.

348   [22]   N. L. Manuel, N. İnanç, M. Lüy, "Control and performance analyses of a DC motor using optimized PIDs and fuzzy logic
349   controller", Results in Control and Optimization, Volume 13, 2023, 100306.

350   [23]   Y. Zhang, X. Xiao, "Fuzzy PID control system optimization and verification for oxygen-supplying management in live fish
351   waterless transportation", Information Processing in Agriculture, 2023,

Figure 1

General structure of ISCS
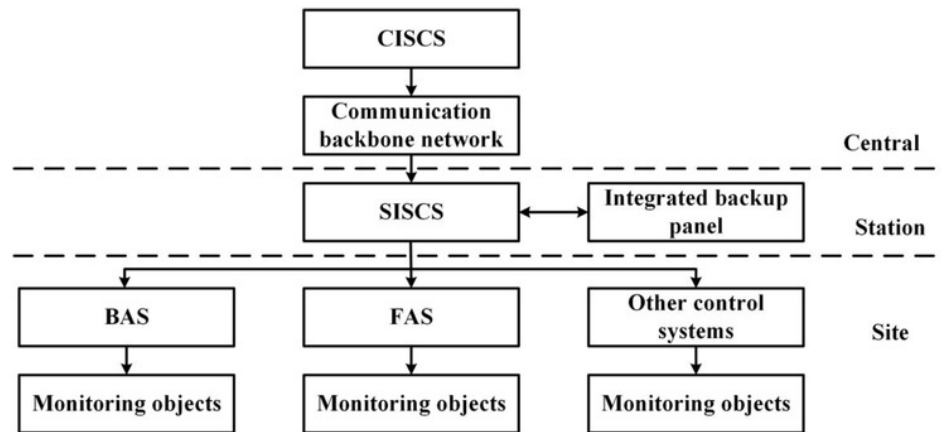
Figure 2

The actual control structure of ISCS
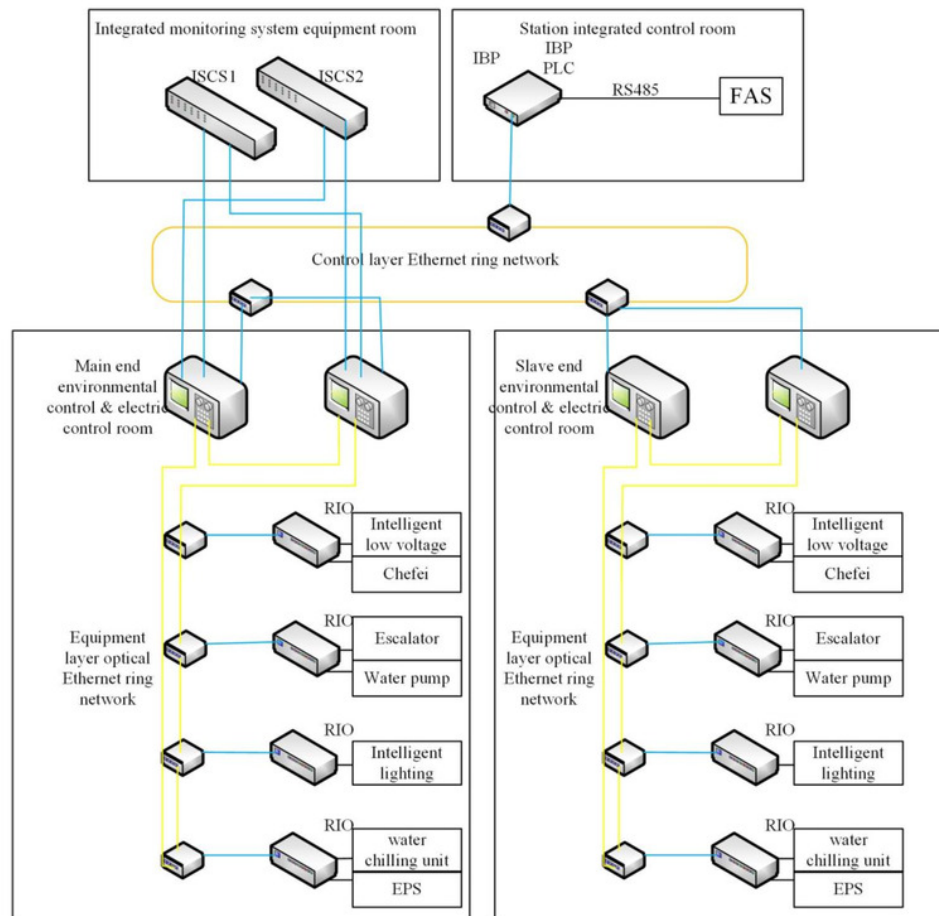
Figure 3

Figure_3
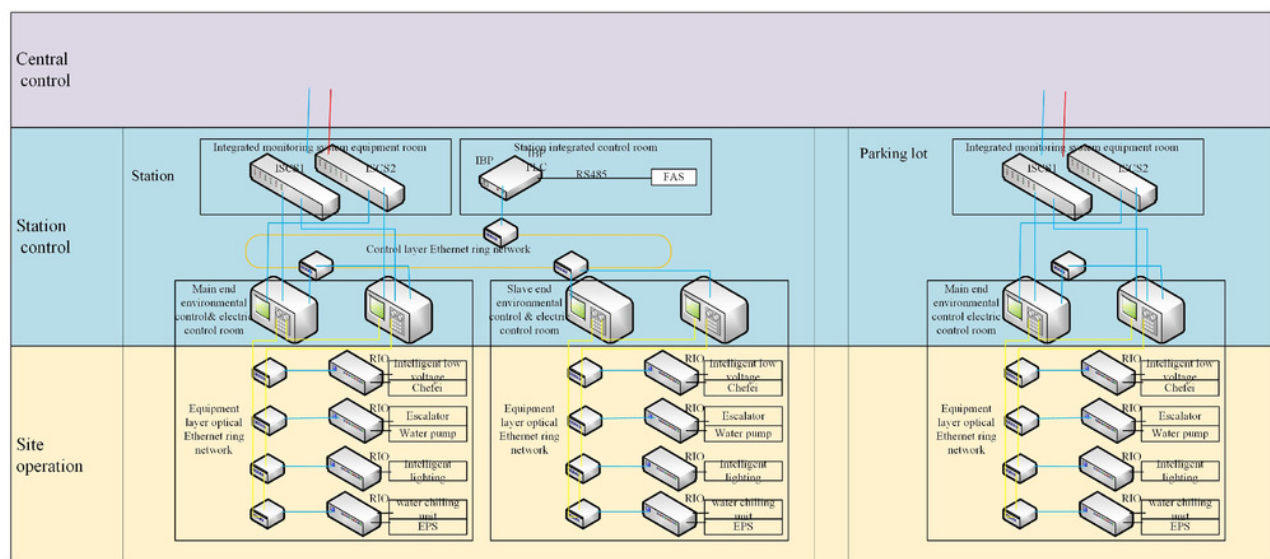
Figure 4

Coordinated control solution architecture for BAS
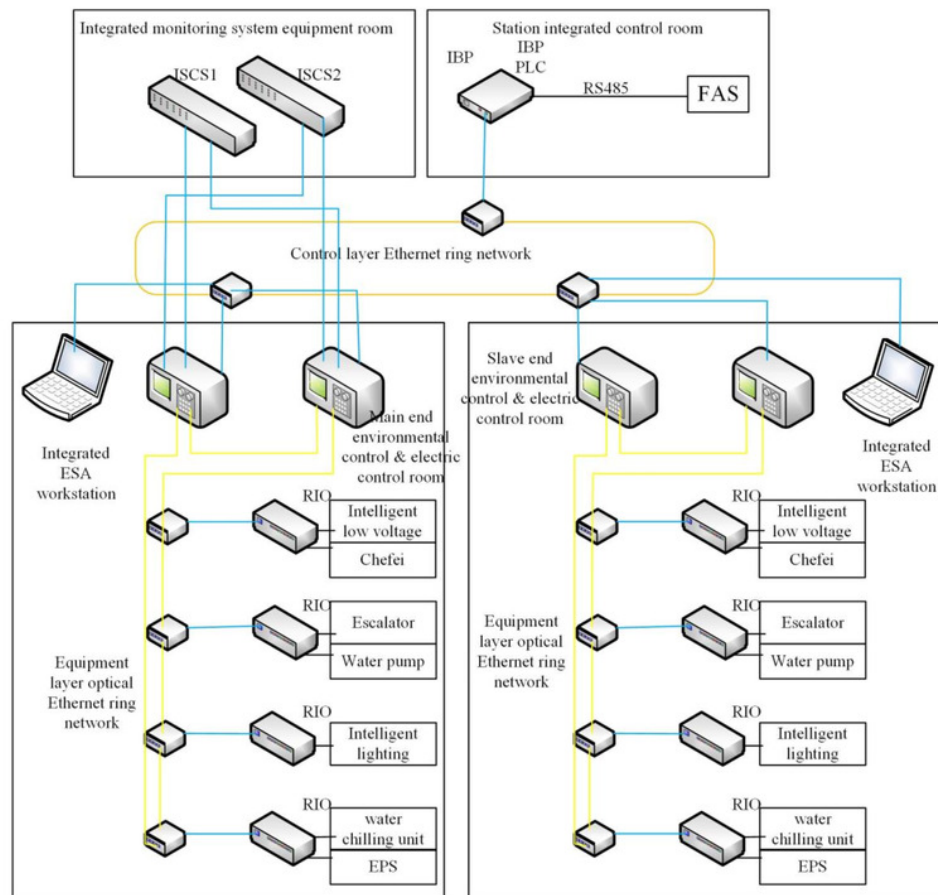
Figure 5

The system structure of the fuzzy PID controller
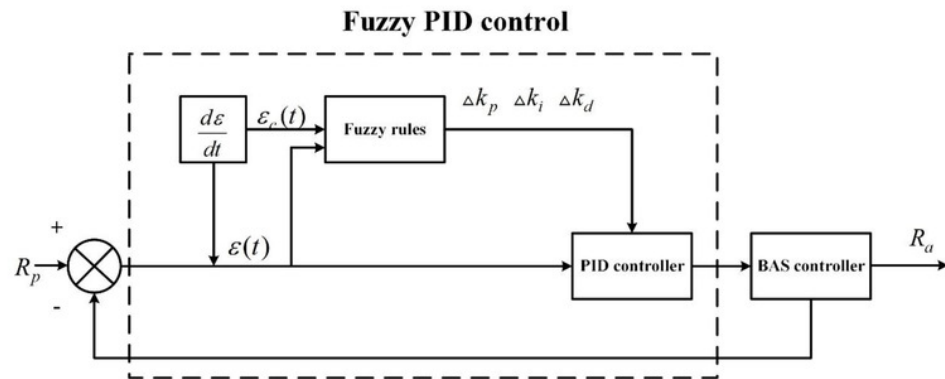
Figure 6

The structure of ISOA-fuzzy PID control-based
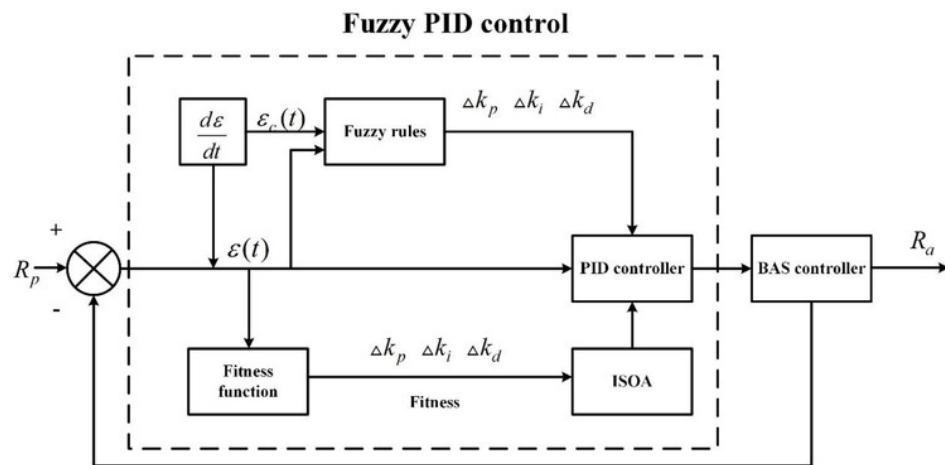
Figure 7

The coordinated control flow of BAS with ISOA-optimized fuzzy PID
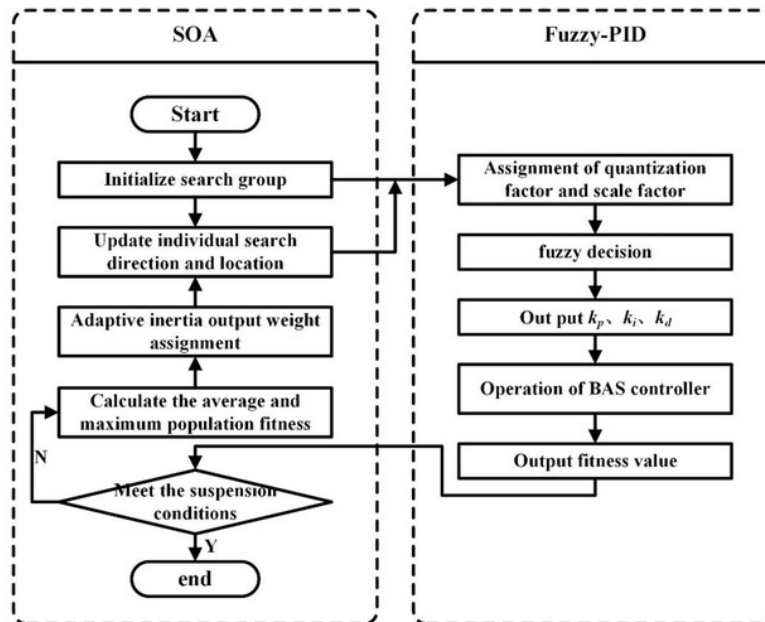
Figure 8

The BAS coordinated control module
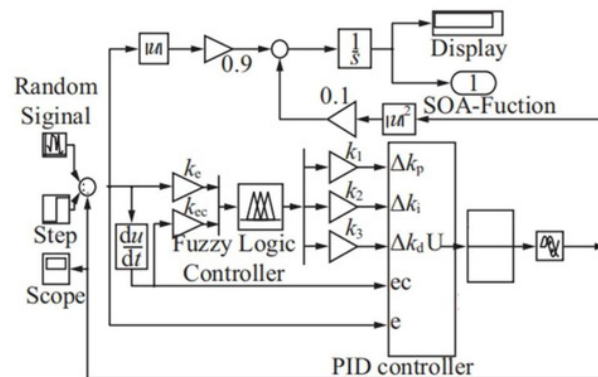
Figure 9

The system response curves for the fuzzy PID, SOA-PID, and ISOA-PID control methods
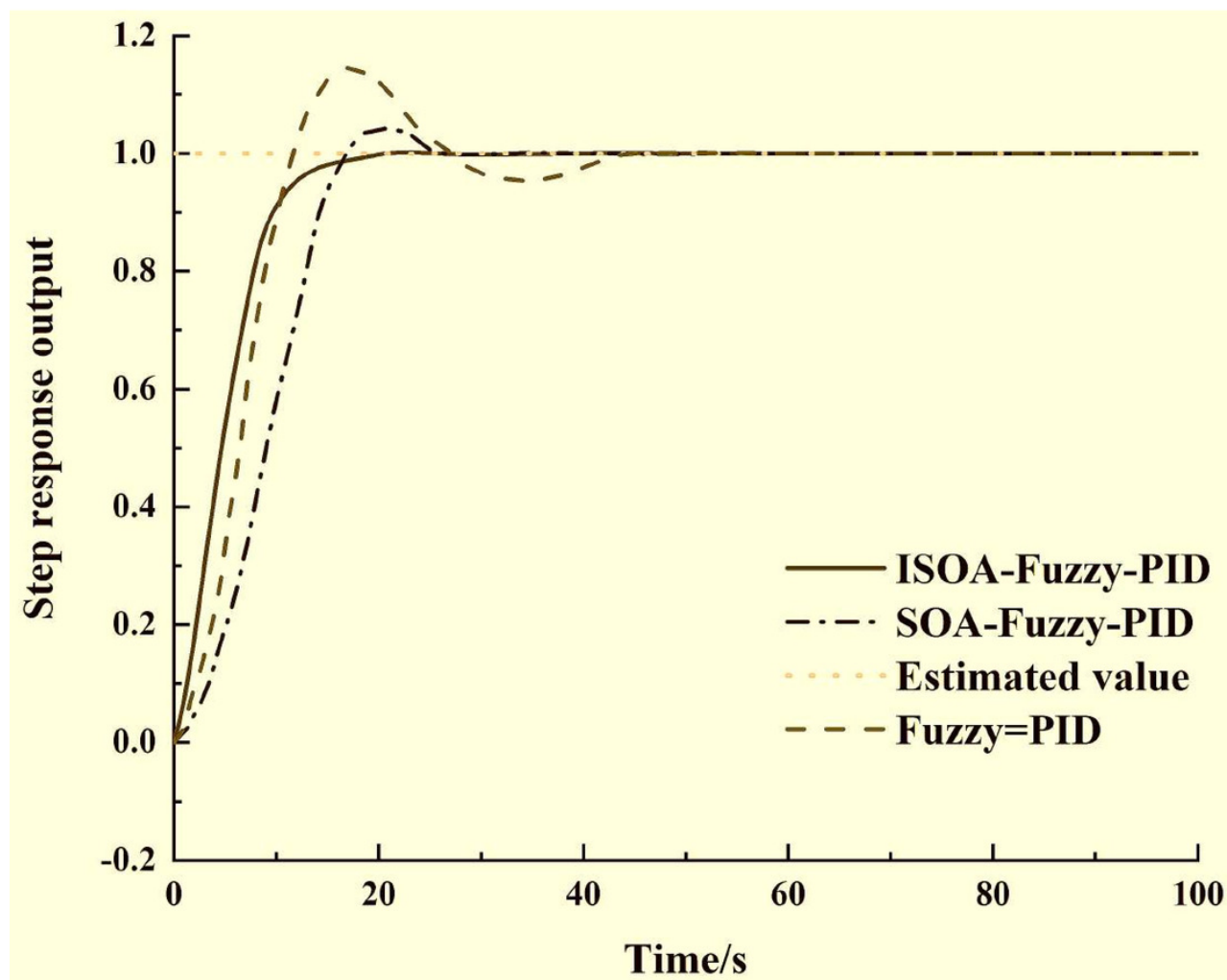
Figure 10

Step response curve of the system with interference
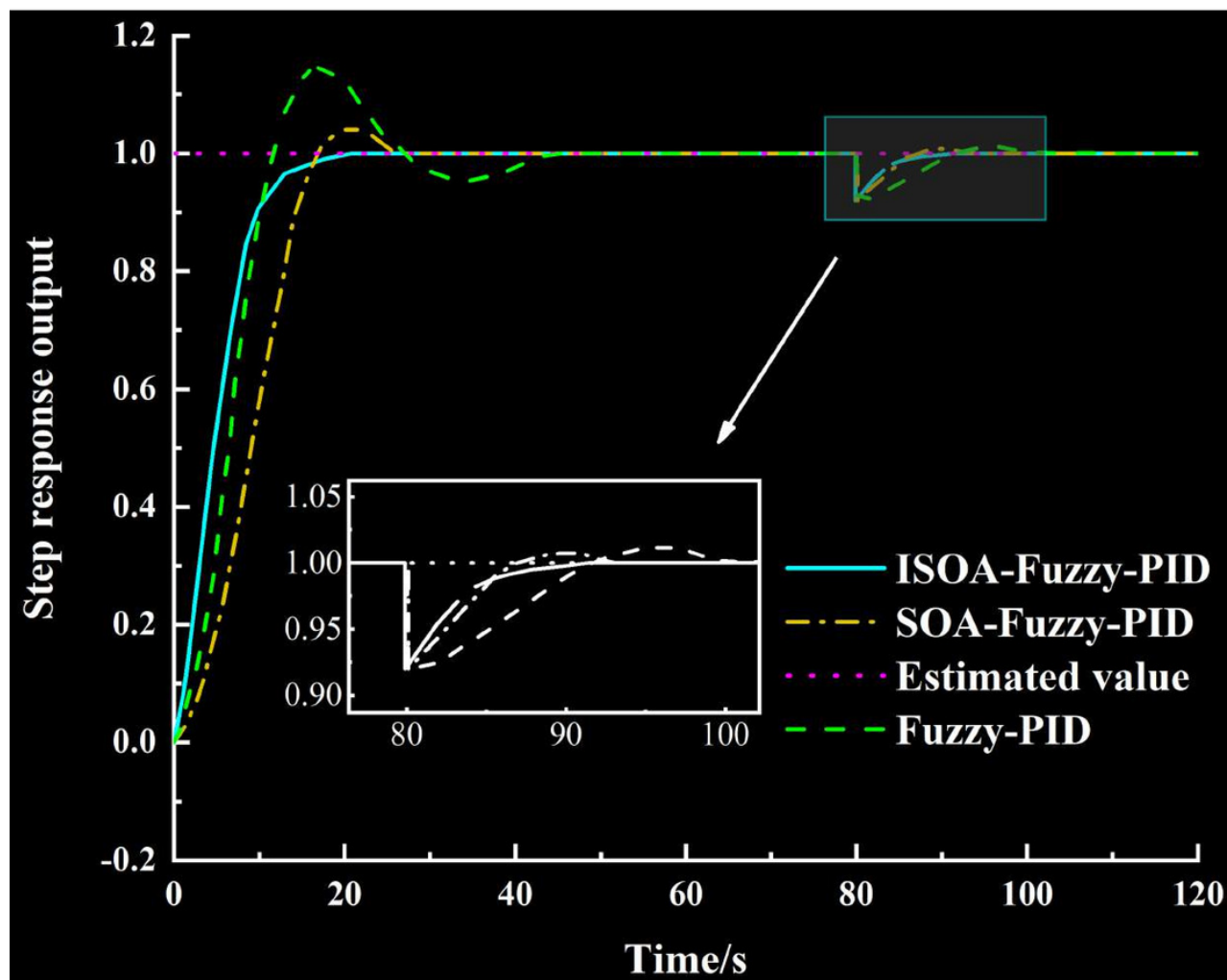
Figure 11

The step response curve of the system with a high-frequency signal
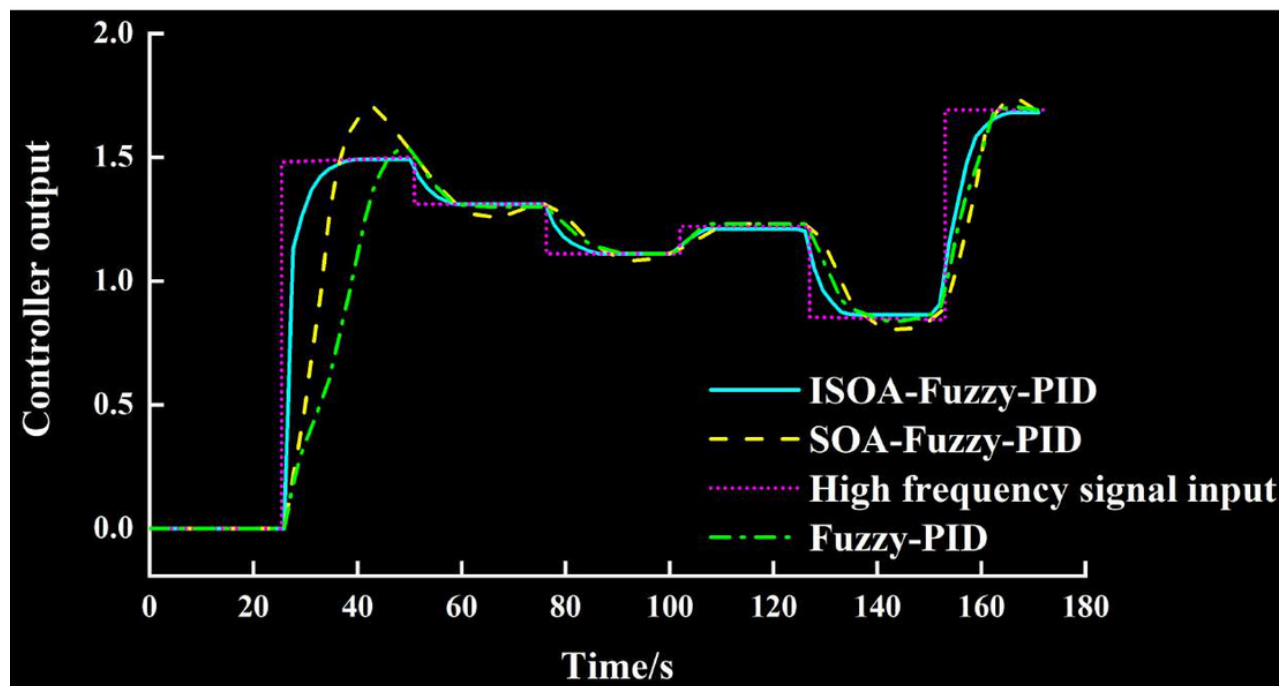
Fuzzy control rule table

$\vee k_p$, $\vee k_i$, $\vee k_d$		ε			
		NB	NM	NS	ZD
ε_c	NB	PB/NB/PS	PB/NB/NS	PM/NM/NB	PM/NM/NB
	NM	PB/NB/PS	PB/NB/NS	PM/NM/NB	PS /NS /NM
	NS	PM/NB/ZO	PM/NM/NS	PS /NM/NM	PS /NS /NM
	ZO	PM/NB/ZO	PM/NM/NS	PS /NM/NM	PS /NS /NM
	PS	PS /NM/ZO	PS /NS /ZO	PS /PM/PM	NS /PS /PS
	PM	PS /ZO/PB	ZO/ZO/NM	NS /PS /PS	NM/PS /PS
	PB	ZO/ZO/PB	ZO/ZO/PM	NM/PS /PM	NM/PM/PM

$\vee k_p$, $\vee k_i$, $\vee k_d$		ε		
		PS	PM	PB
ε_c	NB	PS /NS /NB	ZO/ZO/NM	ZO/ZO/PS
	NM	PS /NS /NM	ZO/ZO/NM	ZO/NS /PS
	NS	PS /NM/NM	NS /PS /PS	NS /PS /ZO
	ZO	NS /PS /NS	NM/PM/NS	NM/PM/ZO
	PS	NS /PM/PM	NM/PM/ZO	NM/PB/ZO
	PM	NM/PM/PS	NM/PB/PS	NB/PB/PB
	PB	NM/PM/PS	NB/PB/PS	NB/PB/PB

Contrast of various performance indicators of the control system

Method	Overshoot/%	Peak time/s	Adjustment time/s	Steady-state error/%
Fuzzy-PID	14.6	16.9	47.1	0.8
SOA-Fuzzy-PID	4.1	20.3	26.4	0.4
ISOA-Fuzzy-PID	0	19.3	19.1	0.01